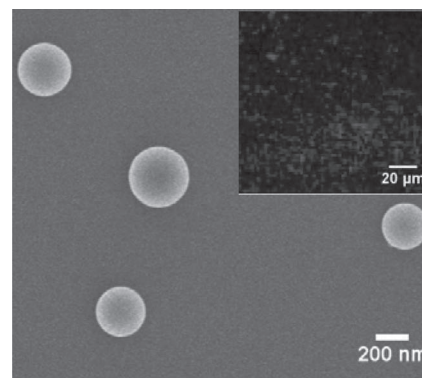


Decomposition-Assembly of Tetraphenylethylene Nanoparticles With Uniform Size and Aggregation-Induced Emission property

Tianxiang Wang, Yunbo Cai, Zhipeng Wang, Erjia Guan, Dahai Yu, Anjun Qin,* Jingzhi Sun, Ben Zhong Tang, Changyou Gao*

Tetraphenylethylene (TPE)-substituted poly(allylamine hydrochloride) (PAH-g-TPE) is synthesized by a Schiff base reaction between PAH and TPE-CHO. The PAH-g-TPE forms micelles in water at pH 6, which are further transformed into pure TPE-CHO nanoparticles (NPs) with a diameter of ≈ 300 nm after incubation in a solution of low pH value. In contrast, only amorphous precipitates are obtained when TPE-CHO methanol solution is incubated in water. The aggregation-induced emission feature of the TPE molecule is completely retained in the TPE NPs, which can be internalized into cells and show blue fluorescence. Formation mechanism of the TPE NPs is proposed by taking into account the guidance effect of linear and charged PAH molecules, and the propeller-stacking manner between the TPE-CHO molecules.



1. Introduction

The nanostructure materials such as nanoparticles (NPs), nanotubes, vesicles, and micelles have attracted considerable attention because of their potential applications in an array of areas, for instance, nano-optoelectronic, biomedical actuators, diagnostic sensors, targeted drug

delivery.^[1–12] In particular, those ones based on organic molecules and self-assembled polymers exhibit not only excellent photoelectronic properties but also great advantages in molecular variety, flexible mechanics, stimuli-responsiveness, and incorporation of functionalities via molecular synthesis.^[13–18] However, unlike their inorganic and metallic counterparts, manipulation of the structures and properties of organic nanostructures are generally difficult due to the limitation of available methods. Moreover, most of the organic building blocks require particular molecular design and synthesis, leading to long steps of routes and low production efficiency.

Very recently, we developed a novel method to obtain one-dimensional nanorods (1D-NRs) or nanotubes (1D-NTs) from poly(allylamine hydrochloride) (PAH)-g-pyrene (Py) microcapsules (MCs).^[19] These 1D-NRs or 1D-NTs are composed of 1-pyrenecarboxaldehyde (Py-CHO) through π - π stacking self-assembly during the hydrolysis of Schiff base bonds between PAH and Py-CHO in acidic

T. Wang, Y. Cai, Z. Wang, E. Guan, D. Yu, A. Qin, J. Sun, B. Z. Tang, C. Gao
MOE Key Laboratory of Macromolecular Synthesis and Functionalization, Department of Polymer Science and Engineering, Zhejiang University, Hangzhou 310027, China
E-mail: qinaj@zju.edu.cn; cygao@mail.hz.zj.cn (CG)
B. Z. Tang
Department of Chemistry, Institute for Advanced Study, The Hong Kong University of Science & Technology, Clear Water Bay, Kowloon, Hong Kong, China

solutions. Formation of the nanostructures is controlled by the structure of polyelectrolytes. For example, the linear polymers such as PAH and poly-L-lysine (PLL) can direct the similar 1D nanostructures formation, but neither the branched polyethyleneimine (PEI) nor the small 1-butylamine molecular can. However, no attempt is paid to other pendent groups except Py-CHO, let alone the possible assembly and new aggregation structures.

Recently, aggregation-induced emission (AIE) phenomenon was discovered and its importance is gradually recognized. The phenomenon is found in a series of propeller-shaped non-planar molecules. Unlike the normal fluorochromes, they are non-emissive in dilute solutions but induced to strongly emit fluorescence when aggregated in poor solutions.^[20–23] The emission is a result of restriction of intramolecular rotations (RIR), as well as inability of packing among molecules through a π - π stacking process because of the propeller shape. Various efforts have been paid to discover a variety of AIE systems and to explore their technological applications especially in optoelectronic and sensing fields by taking advantage of the AIE effect.^[24] Tetraphenylethylene (TPE) is one of the typical AIE molecules. It has the merits of facile synthesis, good stability (except UV irradiation),^[25] accessible functionalization, and high emission efficiency. Several formats of TPE derivatives such as polymer nanoparticles chemically bonded with TPE fluorochromes, polymer colloidal particles,^[26] fluorescent silica nanoparticles (FSNPs) consisting of fluorogenic cores with silica shells have been fabricated so far.^[27] However, no pure nanostructure has been successfully prepared from the AIE molecules.

In this work, taking the advantages of both decomposition-induced assembly and AIE phenomenon, we will explore the possibility to fabricate AIE-active nanostructures by incorporation of TPE moiety. For this context, tetraphenylethylene carboxaldehyde (TPE-CHO) is synthesized and then grafted onto PAH via a Schiff base reaction to obtain PAH-g-TPE (Figure 1). The PAH-g-TPE forms spherical micelles in water, which are then incubated in acidic solution to investigate the formation of nanostructures. Pure TPE NPs emitting blue fluorescence are obtained. On one hand, the study will further substantiate the phenomenon and mechanism of the decomposition-induced assembly by substituting the π - π stacking Py molecule (plane structure) with the propeller-shaped TPE molecule. On the other hand, only by this newly developed decomposition-assembly, the pure TPE NPs composed of only AIE molecules are obtained. These NPs with photo-illuminating property are envisaged to find diverse applications in biochemistry and nanoscience, such as ultra-sensitive assays, high-throughput screening, optoelectronics, and living cell imaging, etc.

2. Experimental Section

2.1. Materials

Poly(allylamine hydrochloride, PAH, $\overline{M}_n \approx 56$ kDa) was purchased from Sigma-Aldrich. HCl solution (10 mol L⁻¹) was purchased from Sinopharm Company and diluted to the desired concentration. TPE-CHO was prepared according to published procedures.^[28] Other chemicals were used as received. The water used in all experiments was prepared via a Millipore Milli-Q purification system and had a resistivity higher than 18.2 M Ω cm.

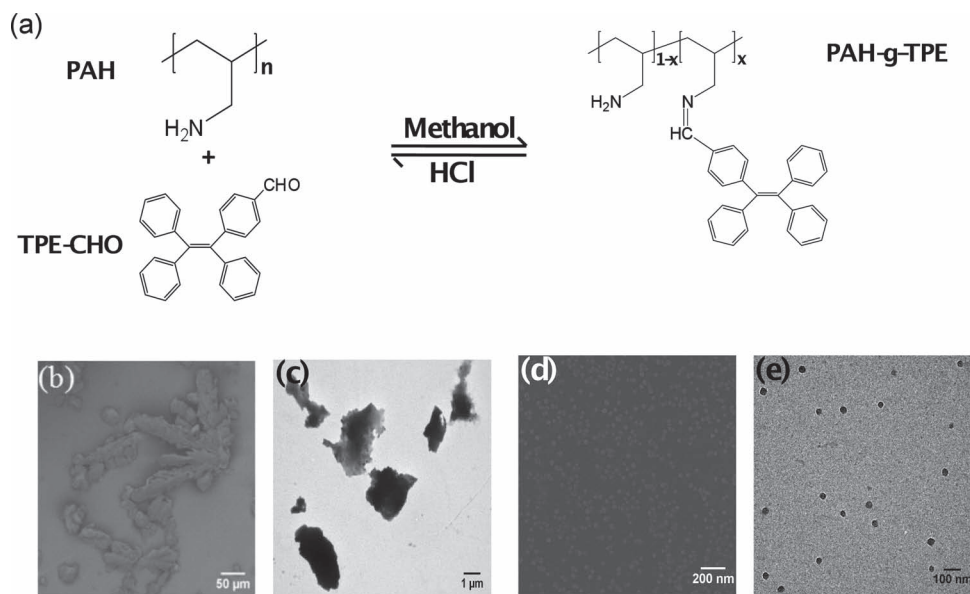


Figure 1. (a) Schematic illustration of reversible formation and decomposition of PAH-g-TPE by reaction between PAH and TPE-CHO. (b,d) SEM and (c,e) TEM images of (b,c) TPE-CHO precipitates obtained in H₂O, and (d,e) PAH-g-TPE micelles formed in H₂O.

2.2. Synthesis of PAH-g-TPE

2 g (0.021 mol repeat unit) PAH was added into 50 mL methanol having 6 g potassium hydroxide. The solution was stirred at room temperature until PAH was dissolved. After the precipitated potassium chloride was filtrated, the filtrate was sealed in a dialysis bag (cut off $\bar{M}_w = 3.5$ kDa) and dialyzed in methanol to remove the excess potassium hydroxide. Finally, the PAH methanol solution (20 mg/mL) was obtained.

8 mg (0.022 mmol) TPE-CHO was dissolved in 2 mL methanol and added into 1 mL PAH methanol solution. The mixture was kept at room temperature for about 10 h to ensure complete reaction between PAH and TPE-CHO, and then kept at 4 °C. The TPE substitution degree was calculated to be 9.73% from ^1H nuclear magnetic resonance (^1H NMR) spectra.

2.3. PAH-g-TPE Micelles Formation

The as-prepared PAH-g-TPE methanol solution was diluted with Millipore water to a methanol/water ratio of 1:4 at pH 6. The micelles were formed in this solution spontaneously and were kept at 4 °C before use.

2.4. TPE-CHO Nanoparticles (TPE NPs) Formation

The as-prepared PAH-g-TPE micelles solution was diluted with HCl solution (pH = 2) to a ratio of 1:4, which was maintained in a vessel for about 24 h. The spherical NPs were formed in this solution and washed with Millipore water by centrifugation to remove free PAH from the solution and to get the TPE NPs. The purified solution was kept at room temperature for further analyses.

2.5. Characterizations

2.5.1. Nuclear Magnetic Resonance Spectroscopy

The ^1H NMR spectra were recorded on Bruker DMX500 equipment by using CD_3OD as the solvent.

2.5.2. Scanning Electron Microscopy

Scanning electron microscopy (SEM) was recorded on a field emission SEM (HITACHI S-4800) at an acceleration voltage of 3 kV. Samples were prepared by placing a drop of the particles suspensions onto a clean glass or silicon wafer and then naturally drying, respectively.

2.5.3. Transmission Electron Microscopy

Transmission electron microscopy (TEM) images were recorded by a JEM-1230 TEM. Samples were prepared by placing a drop of the particles suspensions onto a carbon film-coated copper grid and then naturally drying.

2.5.4. Fluorescence Emission Spectra

Fluorescence emission spectra (FL) were recorded with LS55 (Perkin Elmer). The excitation wavelength was set at 350 nm.

2.5.5. Dynamic Light Scattering and Zeta Potential

Dynamic light scattering (DLS) and zeta potential were measured on a Zeta Potential/Submicron Size Analyzer (Beckman Coulter Delsa Nano C, USA). Each value was averaged from five parallel measurements.

3. Results and Discussion

The PAH-g-TPE molecule was synthesized by grafting TPE-CHO via a Schiff base reaction in methanol as shown in Figure 1a. The formed Schiff base bond is known to be decomposed at acidic condition, releasing the TPE-CHO molecule, which will be accumulated into some structures due to hydrophobic interaction. ^1H NMR spectroscopy (Figure 2) shows that both the resonance peaks assigned to PAH (2.61, 1.58, 1.21 ppm) and TPE-CHO (6.96 and 7.63 ppm) appeared in the PAH-g-TPE molecule except of the aldehyde peak at 9.86 ppm, confirming the successful synthesis of PAH-g-TPE. According to the peak integrals of TPE and PAH, the TPE substitution degree is deduced to be 9.73%, which is almost equal to the theoretical value (10%), conveying the complete reaction between TPE-CHO and PAH. FTIR spectra (Figure S1, Supporting Information) demonstrate the formation of Schiff base (1642 cm^{-1} for $\text{C}=\text{N}$ vibration) in PAH-g-TPE molecule, accompanying with

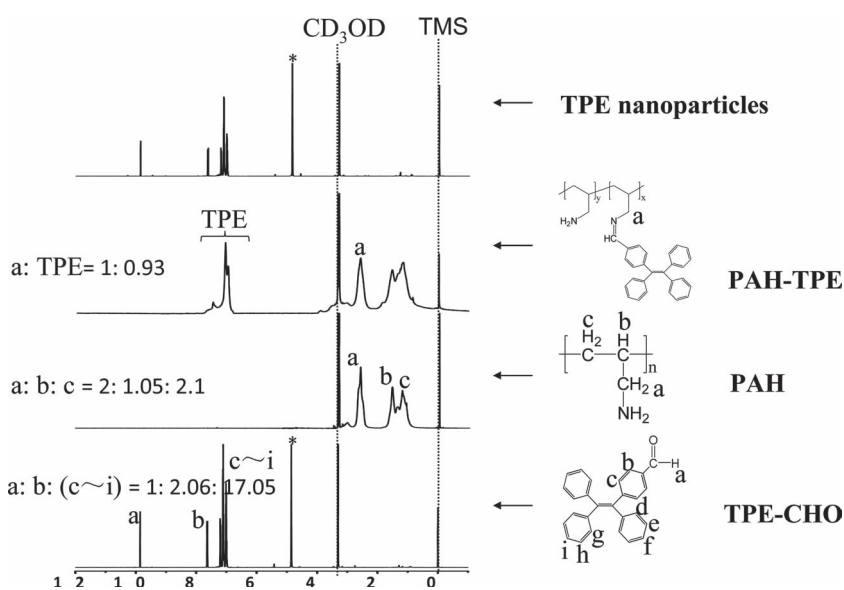


Figure 2. ^1H NMR spectra of TPE-CHO, PAH, PAH-g-TPE, and TPE NPs measured in CD_3OD . The water peak is marked with asterisk.

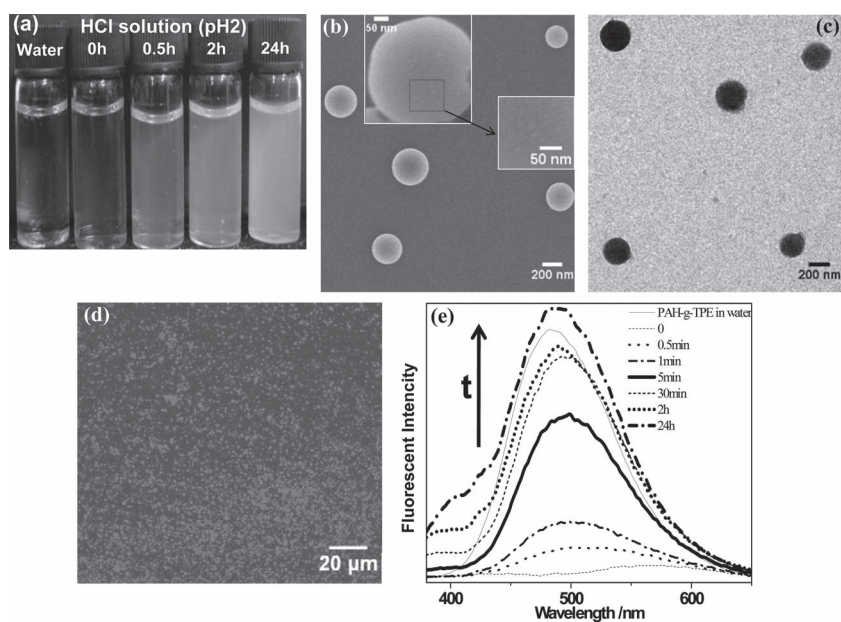


Figure 3. (a) Photo of PAH-g-TPE solution before (water) and after incubation in HCl (pH 2) solution for different time as noted. (b) SEM and (c) TEM images of TPE NPs obtained in pH 2 solution (inset, higher magnification images). (d) CLSM image of TPE NPs obtained in pH 2 solution. (e) Monitoring the formation process of TPE NPs by fluorescence emission spectroscopy, which was recorded immediately upon addition of pH 2 HCl solution ($t = 0$) until 24 h.

After purification by a centrifugation/washing protocol, the obtained colloids were found to be uniform NPs with a size of 300 nm (Figure 3b and c and Figure S2, Supporting Information) regardless of the reaction pH values (2 and 0). These spherical NPs are in good regularity in terms of their shape and size with a smooth surface. No hollow structure was observed by TEM. Moreover, unlike the counterpart particles of normal fluorochromes such as fluorescein and rhodamine, which are readily quenched in a solid state, these TPE NPs emitted blue light (Figure 3d) when excited at 405 nm due to the AIE effect.^[24] This emission was further confirmed by fluorescence spectroscopy (Figure 3e). The emission peaked around 480 nm intensifies along with the incubation time, and eventually surpasses the value of the original PAH-g-TPE micelles, which emit strong fluorescence too.

disappearance of aldehyde group at 1699 cm^{-1} . The asymmetric and symmetric stretching vibration of CH_2 at 2914 and 2849 cm^{-1} is indicative of PAH in the molecule.

Unlike the TPE-CHO that formed amorphous precipitates after being transferred from methanol solution to water (Figure 1b and c), the amphiphilic PAH-g-TPE formed uniform micelles with an average diameter of 34 nm after it was transferred from methanol to an aqueous solution (pH 6, Figure 1d and e). The size is found larger ($\approx 67\text{ nm}$) by DLS, which is attributed to the hydrophilic PAH hairs on the micelle surface. The surface residence of PAH was further confirmed by zeta-potential ($\approx +40\text{ mV}$). The Schiff base is a reversible chemical bond between aldehyde and amino groups. It is stable in neutral and alkaline solutions, but decomposes in acidic solution.^[19,29] Figure 3a shows that the original PAH-g-TPE micelles solution had a very light yellow color with good transparency. The color was changed to pale yellow immediately after the solution pH was decreased to 2 due to the protonation of Schiff base bonds. Along with the time prolongation at this pH, the color faded gradually and the solution became turbid in response to the hydrolysis of PAH-g-TPE. 0.5 h later, the turbidity was rather severe, leading to poor transparency. After 24 h, emulsion with light yellow was formed. The reaction could take place similarly at a pH value of 0, but it was required pretty long time, for example 7 d to yield the same emulsion solution due to the slower decomposition rate of the Schiff base.^[19,29]

The obtained NPs were subjected to characterization by ^1H NMR spectroscopy (Figure 2), FTIR spectroscopy (Figure S1, Supporting Information) and elemental analysis. The NPs and TPE-CHO have identical ^1H NMR spectrum in terms of both the peak positions and intensity, and re-appearance of the peak at 9.86 ppm assigned to aldehyde. No resonance peak assigned to PAH was found. FTIR spectroscopy confirms that the peak of $\text{C}=\text{N}$ at 1642 cm^{-1} as well as the peaks at 2914 and 2849 cm^{-1} disappeared, while the aldehyde peak at 1699 cm^{-1} reappeared. Moreover, elemental analysis revealed that the molar ratio of C/H (1.33) of NPs is close to that (1.34) of TPE-CHO. Nearly no N element was detected, suggesting the complete cleavage of the Schiff base bonds and release of PAH. The change of zeta potential from positive ($\approx +40\text{ mV}$) to negative ($-10.8 \pm 3.5\text{ mV}$) is in good accordance with the pure TPE-CHO structure too. All the results demonstrate that the NPs are purely accumulated from TPE-CHO molecules with neglectable amount of PAH.

The TPE NPs are reasonably formed via the hydrolysis of Schiff base, as confirmed by UV-Vis characterization (Figure. S3, Supporting Information). PAH-g-TPE in methanol and water (micelles) shows maximum absorption at 325 nm, which is similar to that of other TPE derivatives^[30,31] and is attributed to the aromatic conjugated structure of TPE. Upon incubation of the PAH-g-TPE micelles solution in a pH 0 solution here for the sake of sufficient time of monitoring a solution with a lower pH value was adopted. For detail on the reaction kinetics, see

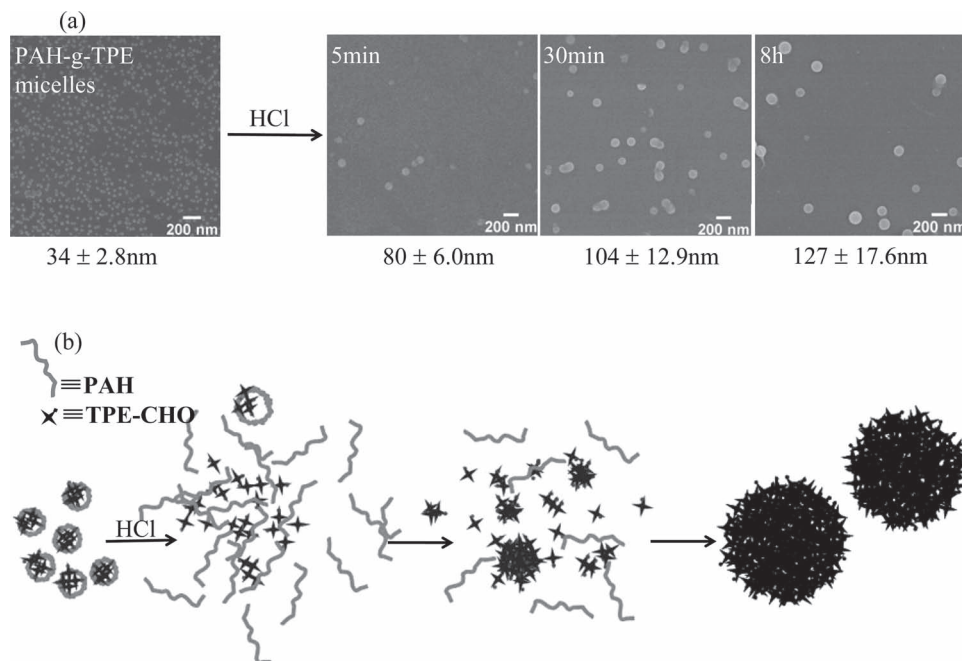


Figure 4. (a) SEM images showing the growth process of TPE NPs as a function of reaction time. (b) Proposed mechanism for TPE NPs formation.

refs.^[19,29]), the peak at 325 nm immediately red-shifted to 388 nm as a result of protonation of the Schiff base bonds. The peak at 388 nm decreased gradually and disappeared after 10 min, accompanying with emergence of absorption at 360 nm. This alteration is in good agreement with the fluorescence emission spectroscopy (Figure 3e) and can thereby explain the instantaneous quenching of 480 nm and weak emission at 550 nm as a result of protonation of Schiff base. The steady enhancement of the emission intensity at 480 nm is caused by the well-known AIE effect, suggesting the gradual increase of degree of accumulation, which inhibits molecular free rotation and thereby the non-irradiative emission.^[32,33] This alteration process also reveals unambiguously the hydrolysis of PAH-g-TPE.

Taking into account the above results, one can deduce that the TPE NPs are not directly formed by accumulation of the micelle cores, since in this case, the emission should not be changed largely. In contrast, they are most probably formed by accumulation of gradually decomposed TPE-CHO molecules around those initially formed seeds, which are stabilized by the surrounding PAH molecules. Monitoring the process of NPs formation by SEM (Figure 4a) consolidates this postulation. It reveals clearly that the initially formed particles have a smaller size of 80 nm (at 5 min reaction), which gradually grow bigger along with prolongation of the reaction time. Finally, after sufficient incubation and thereby decomposition of the Schiff base, TPE NPs with a nice spherical shape and uniformity

are achieved. Based on all the results, the mechanism for formation of the TPE NPs is suggested (Figure 4b). Upon the amphiphilic PAH-g-TPE, micelles are treated in acid solution, the Schiff base bonds are protonated instantaneously, leading to their successive decomposition. This decomposition, however, is lasted for a certain period of time depending on the solution pH. Taking into account, the grafting percentage of TPE ($\approx 10\%$) and the molecular weight of PAH (56 kDa, repeating unit ≈ 600), each PAH-g-TPE contains around 60 TPE molecules. There is no way that all the TPE molecules are cut off simultaneously. In contrast, they should leave the PAH-g-TPE molecule in a time-dependent manner. Hence, the partially hydrolyzed PAH-g-TPE molecule would preferably reside on the initially formed TPE-CHO seeds (driven by hydrophobic force, e.g., π - π stacking) due to its amphiphilic property and act as a stabilizer against formation of large aggregates or precipitates. Along with the progressive hydrolysis, more liberated TPE-CHO molecules will accumulate onto the seeds and finally form the TPE NPs.

Unlike the disc-like planar pyrene (Py) molecule, which stacks in a plane, the TPE molecule stacks in a propeller manner though they are both driven by the hydrophobic force. This difference in stacking manner can explain the different nanostructures formed, that is, NTs or NRs from PAH-g-Py and spheres from PAH-g-TPE. It is conceivable that the propeller interaction cannot guide the growth of molecules along some unique directions. Therefore, spherical NPs are formed due to the lower surface energy.

4. Conclusions

The NPs of pure TPE-CHO, a molecule showing AIE phenomenon, were successfully prepared for the first time. For this context, PAH-g-TPE polymer with a TPE grafting density of 9.73% was synthesized via a condensation reaction between the amino group of PAH and aldehyde group of TPE-CHO. Micelles were formed after PAH-g-TPE was transformed from methanol to water, which were further transformed into uniform TPE NPs by incubation at low pH to decompose the Schiff base linkages. These spherical TPE NPs illuminated strong blue fluorescence with a maximum emission wavelength of 480 nm. In contrast, only amorphous precipitates were formed if TPE-CHO molecules were transformed from methanol to water. The formation mechanism of TPE NPs, but not other formats of nanostructures, is proposed by taking into account the time-dependent hydrolysis of Schiff base, guidance, and stabilization effects of PAH molecules, and propeller-stacking manner of the TPE-CHO molecules. These TPE NPs are expected to be potential candidates as luminescence sensors and optoelectronic applications for their strong fluorescence and physical structure, as demonstrated by the cellular uptake and in situ sensing ability (Figure S4, Supporting Information).

Supporting Information

Supporting Information is available from the Wiley Online Library or from the author.

Acknowledgements: This work is financially supported by Ph.D. Programs Foundation of Ministry of Education of China (20110101130005), the Natural Science Foundation of China (51120135001), the Ministry of Science, and Technology of China for the Indo-China Cooperation (2010DFA51510), the Zhejiang Provincial Natural Science Foundation of China (Z4090177), and Open Project of State Key Laboratory of Supramolecular Structure and Materials (sklssm201224).

Received: May 10, 2012; Revised: June 9, 2012; Published online: July 5, 2012; DOI: 10.1002/marc.201200324

Keywords: aggregation-induced emission; hydrolysis; nanoparticles; poly(allylamine hydrochloride); tetraphenylethylene carboxaldehyde

- [1] K. J. Zhou, Y. G. Wang, X. N. Huang, L. P. Katherine, D. S. Baran, J. M. Gao, *Angew. Chem. Int. Ed.* **2011**, *50*, 1.
- [2] S. Singhal, S. Nie, M. D. Wang, *Annu. Rev. Med.* **2010**, *61*, 359.
- [3] K. Riehemann, S. W. Schneider, T. A. Luger, B. Godin, M. Ferrari, H. Fuchs, *Angew. Chem.* **2009**, *121*, 886.
- [4] M. E. Davis, Z. Chen, D. M. Shin, *Nat. Rev. Drug Discovery* **2008**, *7*, 771.
- [5] D. Peer, J. M. Karp, S. Hong, O. C. Farokhzad, R. Margalit, R. Langer, *Nat. Nanotechnol.* **2007**, *2*, 751.
- [6] S. Vauthey, S. Santoso, H. Gong, N. Watson, S. Zhang, *Proc. Natl. Acad. Sci. U.S.A.* **2002**, *99*, 5355.
- [7] S. Zhang, D. M. Marini, W. Hwang, S. Santoso, *Curr. Opin. Chem. Biol.* **2002**, *6*, 865.
- [8] T.F.A. De Greef, M. M. J. Smulders, M. Wolffs, A. P. H. J. Schenning, R. P. Sijbesma, E. W. Meijer, *Chem. Rev.* **2009**, *109*, 5687.
- [9] E. G. Bellomo, M. D. Wyrsta, L. Pakstis, D. J. Pochan, T. J. Deming, *Nat. Mater.* **2004**, *3*, 244.
- [10] M. Reches, E. Gazit, *Science* **2003**, *300*, 625.
- [11] Y. Wu, J. Xiang, C. Yang, W. Lu, C. M. Lieber, *Nature* **2004**, *430*, 61.
- [12] J. F. Wang, M. S. Gudiksen, X. F. Duan, Y. Cui, C. M. Lieber, *Science* **2001**, *293*, 1455.
- [13] L. Zang, Y. Che, J. S. Moore, *Acc. Chem. Res.* **2008**, *41*, 1596.
- [14] P. Liu, R. Ni, A. K. Mehta, W. S. Childers, A. Lakdawala, S. V. Pingali, P. Thiyagarajan, D. G. Lynn, *J. Am. Chem. Soc.* **2008**, *130*, 16867.
- [15] P. Terech, R. G. Weiss, *Chem. Rev.* **1997**, *97*, 3133.
- [16] F. J. M. Hoeben, P. Jonkheijm, E. W. Meijer, A. P. H. Schenning, *J. Chem. Rev.* **2005**, *105*, 1491.
- [17] A. Ajayaghosh, V. K. Praveen, *Acc. Chem. Res.* **2007**, *40*, 644.
- [18] a) A. Ajayaghosh, V. K. Praveen, C. Vijayakumar, *Chem. Soc. Rev.* **2008**, *37*, 109; b) H. N. Kim, Z. Q. Guo, W. H. Zhu, J. Y. Yoon, H. Tian, *Chem. Soc. Rev.* **2011**, *40*, 79.
- [19] Z. P. Wang, H. Möhwald, C. Y. Gao, *ACS Nano* **2011**, *5*, 3930.
- [20] J. D. Luo, Z. L. Xie, J. W. Y. Lam, L. Cheng, H. Y. Chen, C. F. Qiu, H. S. Kwok, X. W. Zhan, Y. Q. Liu, D. B. Zhu, B. Z. Tang, *Chem. Commun.* **2001**, 1740.
- [21] H. Tong, Y. N. Hong, Y. Q. Dong, M. Haussler, J. W. Y. Lam, Z. Li, Z. F. Guo, Z. H. Guo, B. Z. Tang, *Chem. Commun.* **2006**, 3705.
- [22] H. Tong, Y. N. Hong, Y. Q. Dong, M. Haussler, Z. Li, J. W. Y. Lam, Y. P. Dong, H. H. Y. Sung, I. D. Williams, B. Z. Tang, *J. Phys. Chem. B* **2007**, *111*, 11817.
- [23] Y. N. Hong, M. Haussler, J. W. Y. Lam, Z. Li, K. K. Sin, Y. Q. Dong, H. Tong, J. Z. Liu, A. J. Qin, R. Renneberg, B. Z. Tang, *Chem. Eur. J.* **2008**, *14*, 6428.
- [24] Y. N. Hong, J. W. Y. Lam, B. Z. Tang, *Chem. Soc. Rev.* **2011**, *40*, 5361.
- [25] G. X. Huang, B. D. Ma, J. M. Chen, Q. Peng, G. X. Zhang, Q. H. Fan, D. Q. Zhang, *Chem. Eur. J.* **2012**, *18*, 3886.
- [26] a) W. Qin, D. Ding, J. Z. Liu, W. Z. Yuan, Y. Hu, B. Liu, B. Z. Tang, *Adv. Funct. Mater.* **2012**, *22*, 771; b) C. M. Xing, J. W. Y. Lam, A. J. Qin, Y. Dong, M. Haussler, W. T. Yang, B. Z. Tang, *Polym. Mater. Sci. Eng.* **2007**, *96*, 418.
- [27] M. Faisal, Y. Hong, J. Liu, Y. Yu, J. W. Y. Lam, A. J. Qin, P. Lu, B. Z. Tang, *Chem. Eur. J.* **2010**, *16*, 4266.
- [28] R. R. Hu, J. L. Maldonado, M. Rodriguez, C. M. Deng, C. K. W. Jim, J. W. Y. Lam, M. M. F. Yuen, G. Ramos-Ortiz, B. Z. Tang, *J. Mater. Chem.* **2012**, *22*, 232.
- [29] E. H. Cordes, W. P. Jencks, *J. Am. Chem. Soc.* **1963**, *85*, 2843.
- [30] A. J. Qin, L. Tang, J. W. Y. Lam, C. K. W. Jim, Y. Yu, H. Zhao, J. Z. Sun, B. Z. Tang, *Adv. Funct. Mater.* **2009**, *19*, 1891.
- [31] K. H. Cheng, Y. C. Zhong, B. Y. Xie, Y. Q. Dong, Y. N. Hong, J. Z. Sun, B. Z. Tang, K. S. Wong, *J. Phys. Chem. C* **2008**, *112*, 17507.
- [32] Y. Q. Dong, J. W. Y. Lam, A. J. Qin, Z. Li, J. Z. Sun, H. H.-Y. Sung, I. D. Williams, B. Z. Tang, *Chem. Commun.* **2007**, 40.
- [33] L. D. Lu, R. Helgeson, R. M. Jones, D. McBranch, D. Whitten, *J. Am. Chem. Soc.* **2002**, *124*, 483.